

PRELIMINARY SPH MODELLING OF OXIDE FORMATION DURING THE MOULD FILLING PHASE IN DC CASTING OF EXTRUSION BILLETS

Mahesh PRAKASH^{#1}, Joseph HA^{#1}, Paul W. CLEARY^{#1} and John GRANDFIELD^{#2}

[#]CAST Cooperative Research Centre,

¹CSIRO Mathematical and Information Sciences, Clayton, VIC 3169

²CSIRO Manufacturing and Materials Technology, Preston, VIC 3072

ABSTRACT

Direct chill (DC) casting is widely used to produce aluminium ingots and billets. One of the issues with such castings is the oxide generated especially during the filling of the casting table in the start-up phase. This oxide can affect the performance of the product during subsequent extrusion. While the very first material is cut off and discarded the distribution of oxides along the cast length is not known. It is therefore highly desirable to have an ability to predict the amount and distribution of the oxide generated during the process start-up. In this paper, we use the mesh-free Smoothed Particle Hydrodynamics (SPH) method to model the mould filling phase of DC casting. The free surface nature of the flow during this phase is especially amenable to the mesh-free SPH modelling technique. Additionally this method is very suitable for predicting surface driven and history dependent properties such as oxides. The paper presents preliminary predictions of cumulative interior and exterior oxide levels with time in a typical DC casting operation. The amount of interior oxide will indicate the effect of oxide on the final metal microstructure. The amount of exterior oxide determines the surface quality of the billet.

INTRODUCTION

In direct chill (DC) casting, molten aluminium is poured from the furnace through a troughing system into a refractory mould table placed on water box containing moulds of the desired billet diameter as shown in Figure 1. After filling the starting heads in the mould, the mould descends and the emerging billets are cooled by the direct chill water spray.

During aluminium melt transfer oxides can form which are detrimental to the product quality and cause defects during extrusion. Filters are used in the transfer from the furnace to the DC casting process to remove oxides and other particles. However, filling of the mould table takes place after the filter and during this filling stage oxides can be generated. At present there is no easy way of experimentally evaluating the amount of oxide produced during such operations as a function of table design or filling practice. Thermal related defects can also occur at the start of casting due to too short or too long a mould filling time. Thus, one desires a mould table design which minimizes filling time variation from mould to mould, fills fast enough and does not create turbulence, splashing and oxides. The mould table can have more than 100 billets depending on the diameter.

In the past, modelling of the flow and temperatures during DC casting table filling have been carried out using mesh based methods such as the general purpose FEM code FIDAP (Schneider and Grun, 1995, Grun and Schneider, 1997 and Grun and Schneider, 1998). Smoothed Particle Hydrodynamics (SPH), due to its Lagrangian nature, is well suited to simulating the complex free surface flow, such as found in the DC casting start-up phase. It also has strong advantages in simplifying predictions of oxide generation and transport, allowing estimates to be made of interior and exterior oxide content in a given metal casting system. These advantages have led to the use of SPH in several casting processes including prediction of oxide content and optimization of wheel design in aluminium re-melt ingot casting reported in Cleary et al. (2004) and Prakash et al. (2006), high pressure die-casting in Cleary et al. (2000) and Cleary and Ha (2003) and gravity die casting Ha et al. (1999).

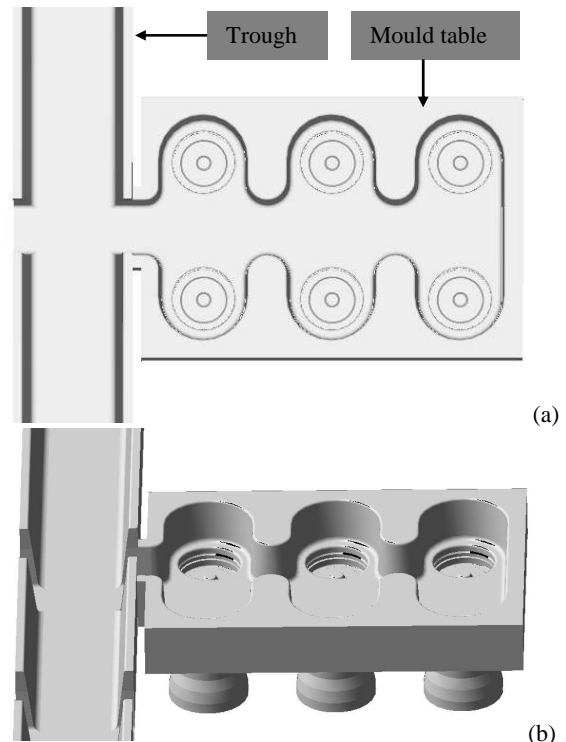


Figure 1: Schematic showing (a) a vertical and (b) a side view of the DC Casting configuration with a trough and mould table containing six moulds.

SPH MODELLING

SPH is a numerical method for modelling coupled fluid flows, solid structures and heat transfer with some unique capabilities. SPH is particle based rather than using conventional fixed grids or meshes to track the fluid and calculate the fluid velocities. The fluid is represented as “blobs” that move around in response to the fluid or solid stresses produced by the interaction with other particles. SPH is particularly well suited to momentum dominated flows, flows involving complex free surface behaviour and flows with complex physics such as solidification or flow through industrial porous media. It is also useful for flows around moving objects, since there are no mesh structures to be affected.

A brief summary of the SPH method is presented here. For more comprehensive details one can refer to Gingold and Monaghan (1977), Monaghan (1992) and Cleary and Monaghan (1999). The interpolated value of a function A at any position \mathbf{r} using SPH smoothing can be written as:

$$A(\mathbf{r}) = \sum_b m_b \frac{A_b}{\rho_b} W(\mathbf{r} - \mathbf{r}_b, h) \quad (1)$$

where m_b and \mathbf{r}_b are the mass and density of particle b and the sum is over all particles b within a radius $2h$ of \mathbf{r} . Here $W(\mathbf{r}, h)$ is a C^2 spline based interpolation or smoothing kernel with radius $2h$, that approximates the shape of a Gaussian function but has compact support. The gradient of the function A is given by differentiating the interpolation equation (1) to give:

$$\nabla A(\mathbf{r}) = \sum_b m_b \frac{A_b}{\rho_b} \nabla W(\mathbf{r} - \mathbf{r}_b, h) \quad (2)$$

Using these interpolation formulae and suitable finite difference approximations for second order derivatives, one is able to convert parabolic partial differential equations into ordinary differential equations for the motion of the particles and the rates of change of their properties.

Continuity equation:

From Monaghan (1992), the SPH continuity equation is:

$$\frac{d\rho_a}{dt} = \sum_b m_b (\mathbf{v}_a - \mathbf{v}_b) \cdot \nabla W_{ab} \quad (3)$$

where ρ_a is the density of particle a with velocity \mathbf{v}_a and m_b is the mass of particle b . We denote the position vector from particle b to particle a by $\mathbf{r}_{ab} = \mathbf{r}_a - \mathbf{r}_b$ and let $W_{ab} = W(\mathbf{r}_{ab}, h)$ be the interpolation kernel with smoothing length h evaluated for the distance $|\mathbf{r}_{ab}|$. This form of the continuity equation is Galilean invariant (since the positions and velocities appear only as differences), has good numerical conservation properties and is not affected by free surfaces or density discontinuities.

Momentum equation:

The SPH momentum equation used here is:

$$\frac{d\mathbf{v}_a}{dt} = \mathbf{g} - \sum_b m_b \left[\left(\frac{P_b}{\rho_b^2} + \frac{P_a}{\rho_a^2} \right) - \frac{\xi}{\rho_a \rho_b} \frac{4\mu_a \mu_b}{(\mu_a + \mu_b)} \frac{\mathbf{v}_{ab} \mathbf{r}_{ab}}{\mathbf{r}_{ab}^2 + \eta^2} \right] \nabla_a W_{ab} \quad (4)$$

where P_a and μ_a are pressure and viscosity of particle a and $\mathbf{v}_{ab} = \mathbf{v}_a - \mathbf{v}_b$. Here ξ is a factor associated with

the viscous term (Cleary, 1996), η is a small parameter used to smooth out the singularity at $\mathbf{r}_{ab} = 0$ and \mathbf{g} is the gravity vector. The first two terms involving the pressure correspond to the pressure gradient term of the Navier-Stokes equation. The next term involving viscosities is the Newtonian viscous stress term.

Equation of state:

Since the SPH method used here is quasi-compressible one needs to use an equation of state, giving the relationship between particle density and fluid pressure. This relationship is given by the expression:

$$P = P_0 \left[\left(\frac{\rho}{\rho_0} \right)^\gamma - 1 \right] \quad (5)$$

where P_0 is the magnitude of the pressure and ρ_0 is the reference density. For water and liquid metals we use $\gamma = 7$. This pressure is then used in the SPH momentum equation (4) to give the particle motion. The pressure scale factor P_0 is given by:

$$\frac{\gamma P_0}{\rho_0} = 100V^2 = c_s^2 \quad (6)$$

where V is the characteristic or maximum fluid velocity. This ensures that the density variation is less than 1% and the flow can be regarded as incompressible.

Oxide modelling:

Aluminium oxide grows on the surface of molten aluminium due to exposure to air. This oxide layer can be broken by flow of the melt creating new surface. The surface may be folded over on itself entraining the oxide films. Any splashing will result in droplets of melt surrounded by oxide film that become dross on the surface melt. To quantify this oxide formation, a linear oxide (O_x) growth model suggested by Baker et al. (1995) is used:

$$\frac{dO_x}{dt} = k_l \quad (7)$$

where k_l is the rate constant and t time. These authors estimated the rate constant to be $k_l = 10.9 \times 10^{-3} \text{ kg/m}^2 \text{ s}$. Note that the oxide is transported with the fluid and no account of any apparent density difference causing the oxide to sink or rise is allowed for.

DC CASTING MODEL SETUP

A unit of 6 moulds was modelled for simplicity. The dimension of the DC casting mould table given in Figure 1 is 0.83 m long and 0.575 m wide with a gate width of 0.114 m. There are six circular moulds in the table each with diameter 0.135 m. The design used is a conceptual one typical of industry practice. A starting head, mounted to a hydraulic ram, forms a false bottom to the mould. When the mould is filled and the metal begins to solidify, the starting head is lowered at a controlled rate. As the starting head lowers, water jets built into the mould spray water onto the billet to cool the surface and further solidify the metal. Multiple moulds in the table contribute to high production rates in the cast house.

The metal height in the launder system is kept constant at 70 mm with respect to the base of the mould table. This pressure head thus controls the flow to the mould table. In practice the metal head depends on the flow rate from

the furnace. To represent this pressure head in the SPH simulation, a reservoir of fluid of fixed height is placed in the launder in front of the gate as shown in Figure 2. A pressure inflow boundary condition of 1614 Pa is applied at the inflow to the reservoir to maintain a steady head of 70 mm while at the same time achieving a mould table fill time of around 30 seconds. The descent of the starting head is not simulated. The model is isothermal.

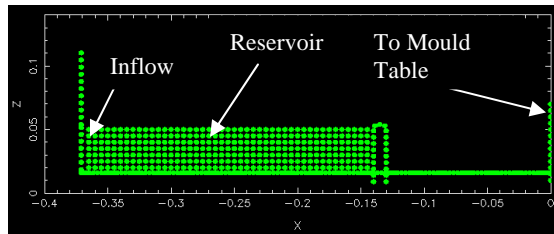


Figure 2: Cross section of the constant head inflow reservoir used to control the inflow to the mould table.

A resolution of 5 mm was used for the particles representing the molten metal, the moulds and mould table. The number of particles used for the geometry is 123,321. The number of fluid particles increases with time as more and more particles are generated by the inflow. The final number of fluid particles when the mould is full is around 120,000.

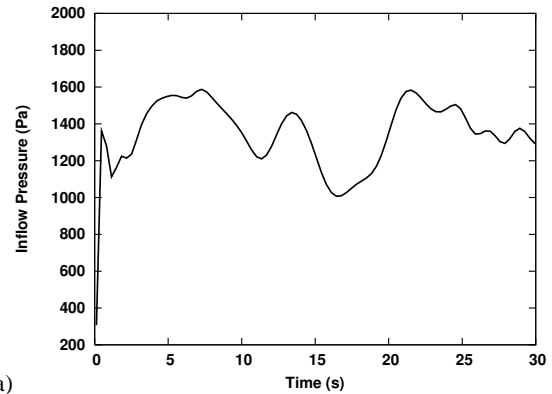
Figure 3 shows the variation of inflow pressure and velocity as it adapts to fluid flow causing a ramp up in pressure to maintain the specified pressure head.

FLOW PATTERN IN DC CASTING TABLE

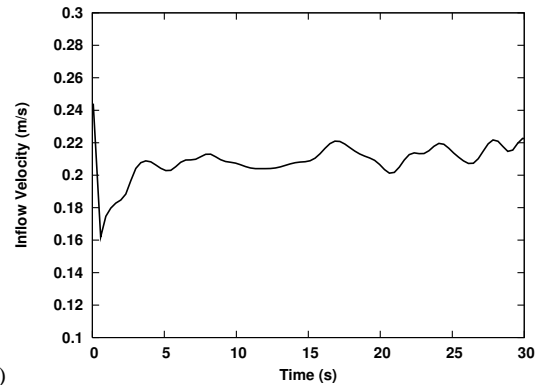
Figure 4 shows the filling of the mould table. The molten metal is coloured by speed in frames on the left and by oxide fraction in the frames on the right. The metal speed is coloured with red being the maximum of 0.21 m/s and blue being stationary. The oxide fraction is coloured with blue representing no oxide content and red representing a maximum of 6.8 $\mu\text{g}/\text{kg}$. At 3.0 s, the metal starts jetting into the table and has a very fragmented structure. There is some metal flowing into the first two moulds but most of it flows forward further into the table at high speed.

At 5.0 s, the molten metal is still very fragmented and the leading material has now hit the end of the DC table. Once the metal hits the end of the table it slows and starts to backfill. The two moulds at the end of the table therefore start filling faster than the other four moulds.

At 7.0 s, the back filling nature of the flow is evident with the two moulds at the end now almost 30 to 40% full. The base of these moulds is almost fully covered by liquid metal. The four other moulds are less than 10% full at this stage. Modest but meaningful oxide levels are now observed close to the centre of the moulds as shown by the pale blue colour of the metal in the right frame.



a)



b)

Figure 3: Variation of inflow pressure (bottom) and velocity (top) and with time.

At 9.0 s, the last two moulds are almost 80% full with metal now starting to backfill the two moulds in the middle of the table. There is a strong central jet of clean new metal coming into the table seen from the red coloured liquid in the centre at this stage. The liquid metal has slowed down considerably on the sides in the moulds as well as at the end leading to the back filling.

At 11.0 s, the backfilling of the middle two moulds is still in progress but the last two moulds at the end of the table are now almost completely full. The length of the central strong jet has started to diminish with this now occupying only one third of the table length.

By 13.0 s the entire surface of the table is covered with metal. By this stage the back filling of the moulds has almost ceased and the strength of the central jet has also reduced considerably.

Between 13.0 and 25.0 s there is no significant change in the metal flow pattern. During this stage the entire surface of the table is covered with metal and the filling consists of a steadily rising depth of metal until it reaches the head level of 70 mm. The largest increase in metal fill level at this stage is for the two moulds at the front. The velocity and oxide distributions on the surface of the metal do not vary significantly during this stage.

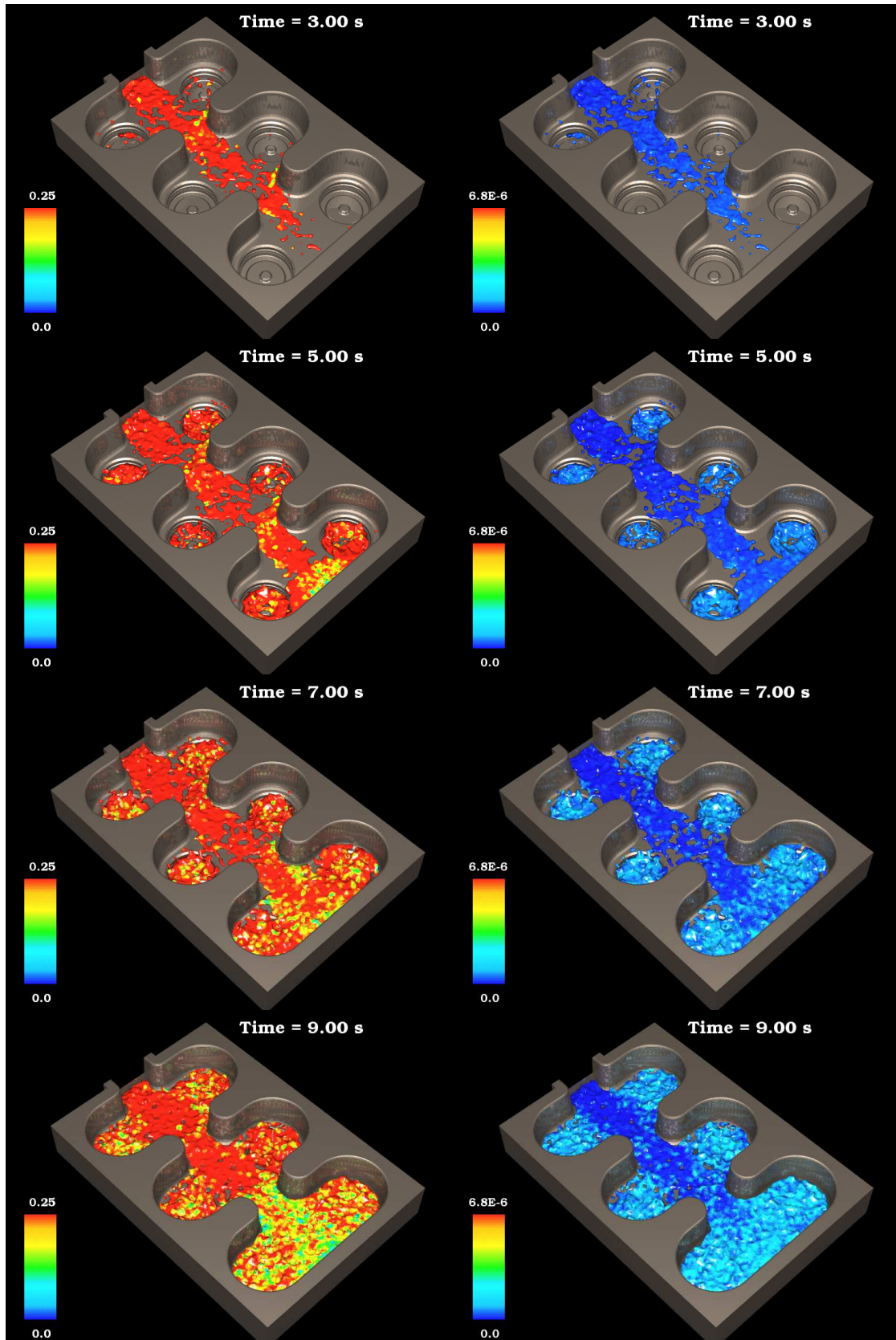


Figure 4: Filling patterns of DC mould table at different times. The fluid is coloured by speed (left column) and by oxide mass (right column).

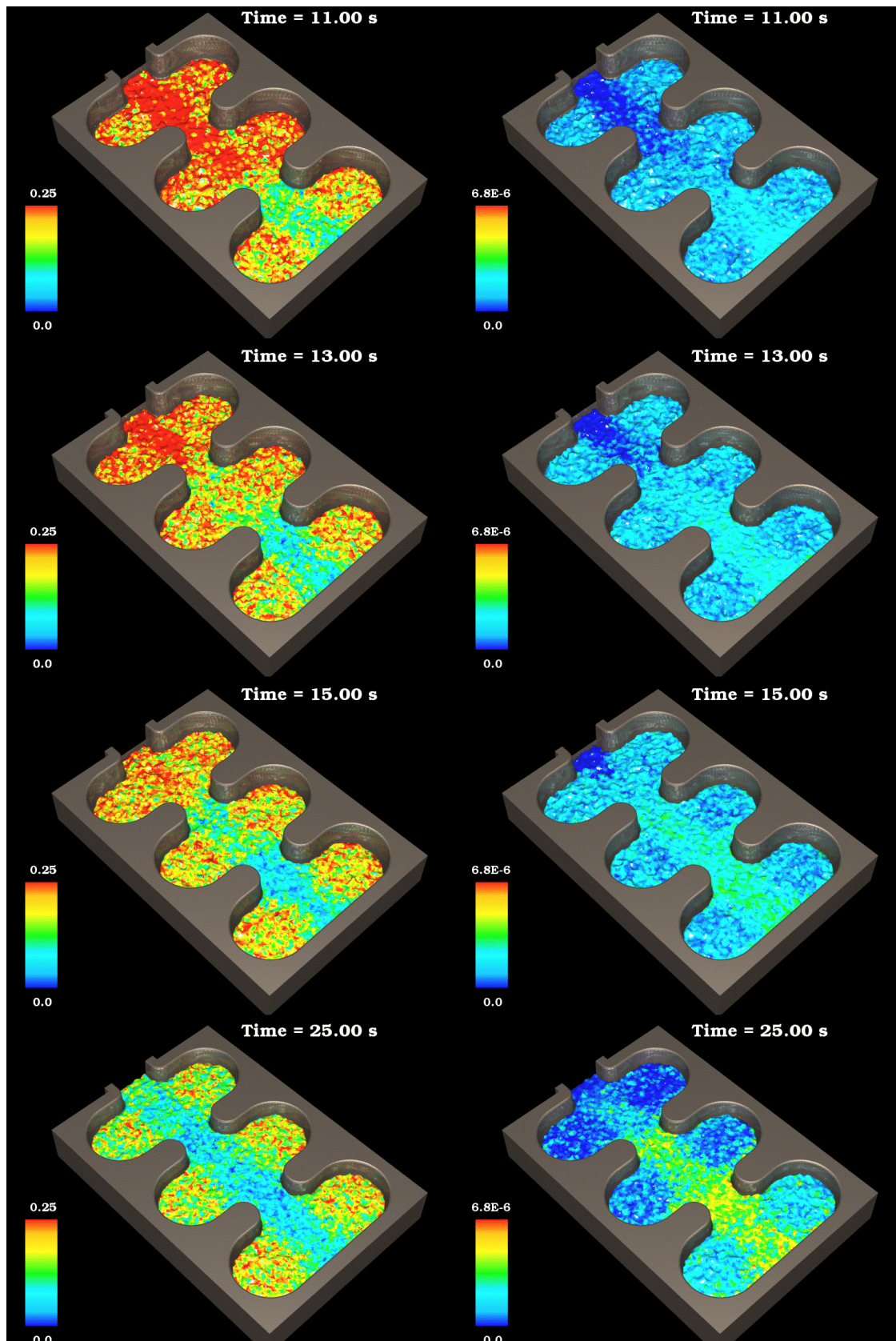


Figure 4: Filling patterns of DC mould table at different times. The fluid is coloured by speed (left column) and by oxide mass (right column).

By 25.0 s, the entire table is filled with the metal depth reaching the required level of 70 mm thus completing the start-up phase of the DC cast process. The central jet of metal has now become weak as indicated by the pale blue colour on the left frames. Higher velocity regions are actually seen in the mould as the metal swirls around as indicated by the yellow to red colour in the six moulds. There is a steady increase of oxide level in the metal mass during this stage as seen by the change in colour of the metal surface from pale blue to yellow.

In general, the amount of oxide in the metal shows a gradual increase from the gate to the end of the table and a decrease from the central region to the sides of the table. Due to the constant head condition the metal flow rate in the central region gradually diminishes as the metal in the table rises up to the requisite level of 70 mm. Due to the low metal flow rate in the central region the amount of oxide in this region is higher as the relatively slow moving metal is exposed to air for a longer time.

Since the metal in the six moulds is moving around in a swirling pattern the oxide produced on the surface becomes entrained into the moulds leading to lower oxide on the exterior moulds as seen from the pale blue colour of metal in the moulds in the right frame at 25.0 s.

As fresh metal flows into the table from the gate, its exposure to the air as it flows down the table causes oxide to form. The metal in the region above the mould is constantly replenished by metal flowing from the central region. In these regions, the flow has a circular pattern with significant mixing. These results suggest that the surface layer of the metal in the central region of the table is the primary location for oxide formation.

OXIDE GENERATED DURING DC CAST FILLING

Figure 5 shows the time variation of the total, interior and exterior oxide in the metal as a percentage of the metal mass in the table. The amount of oxide formed represents only a small fraction of the total metal. However this can be a significant absolute amount when the total aluminium DC cast production is taken into account.

The percentage of total oxide in the metal increases almost linearly with time. By around 20 s the total percentage of oxide reaches a peak value of around 0.31% and then starts to gently decline.

The percentage of external oxide increases rapidly at the start with a level only slightly lower than for the total oxide. This indicates that most of the early oxide is on the surface where it is created. The external oxide percentage reaches a maximum of about 0.15% at around 12 s and then slowly decreases as a proportion of total metal. This is expected since the total surface of the mould table is constant, and thus the maximum surface area of the metal that can be exposed to air, is fixed. At the same time the total amount of metal in mould table increases steadily with time.

The interior oxide curve has a slow rate of increase at first but then increases more rapidly between 12 and 20 s. The total interior oxide content reaches a steady percentage of around 0.25% at 25 s. The steady level of

interior oxide is maintained even with the addition of more metal into the table suggesting that the actual level of interior oxide is increasing with time. This is because the strong levels of mixing in the moulds observed towards the end of the filling process, promotes the entrainment of oxide into the metal interior. The interior oxide can result in possible defects in the billet. The exterior oxide on the other hand has a significant effect on the surface finish of the billet.

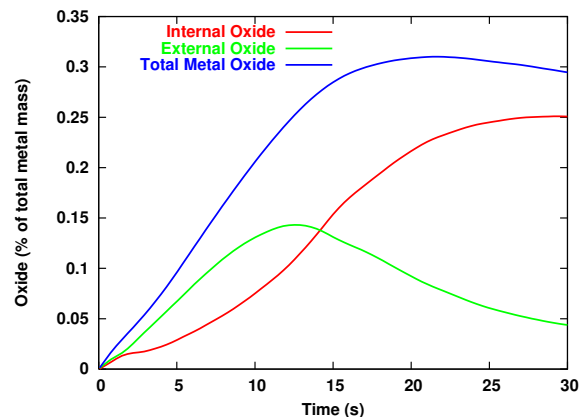


Figure 5: Temporal variation of oxide as percentage of total metal.

CONCLUSIONS

SPH simulation of DC casting gives a detailed prediction of the flow pattern of molten metal from the launder to the mould table, the rate of oxide formation on the exposed metal surface and its subsequent entrainment into the metal.

The Lagrangian nature of SPH makes it simple to track the movement of oxide from its formation on the exposed surface of the molten metal to its mixing into the fluid as the metal flows from the refractory to the mould table through the launder system.

The simulation demonstrates:

- The metal fill pattern in the mould table is strongly dependent on the metal flow speed. Faster metal speeds leads to more back filling whereas slower speeds can lead to a more front filling pattern.
- Exterior and interior oxide in the metal can be predicted during the start-up phase using SPH. Exterior oxide is responsible for the surface finish of the billet whereas interior oxide can affect the metal microstructure. Both properties significantly affect the usability of the final product.
- SPH simulations can be used to evaluate oxide levels and fill patterns for different metal flow rates and mould arrangements in a DC table leading to an optimised DC casting system.

In the next stage we will be comparing the SPH simulation results with water analogue modelling results as well as actual DC casting experimental results using molten metal.

ACKNOWLEDGMENTS

This project was conducted by the CASTcrc. The support of Comalco and ODT Engineering are gratefully acknowledged. CSIRO, Comalco and ODT Engineering are core participants in the CASTcrc, which was established under and is supported in part by the Australian Government's Cooperative Research Centres scheme.

REFERENCES

- BAKER, P.W., NGUYEN, K., KIRKALDIE, R., (1995), in *Aluminium Cast House Technology 4th Australasian Asian Pacific Conference*, TMS, p. 109.
- CLEARY, P., (1996), "New implementation of viscosity: tests with Couette flows." *SPH Technical Note 8, CSIRO DMS, Technical Report DMS – C 96/32*.
- CLEARY, P.W., HA, J. and AHUJA, V., (2000), "High pressure die casting simulation using smoothed particle hydrodynamics." *Int. J. Cast Metals Res*, **12**, 335-355.
- CLEARY, P.W. and HA, J., (2003), "Three-dimensional SPH simulation of light metal components." *J. Light Metals*, 2/3, 169-183.
- CLEARY, P. W. & MONAGHAN, J. J., (1999), "Conduction modelling using smoothed particle hydrodynamics", *J. Computat. Phys.*, **148**, 227-264.
- CLEARY, P., PRAKASH, M., HA, J., SINNOTT, M., NGUYEN, T. and GRANDFIELD, J., (2004), "Modelling of cast systems using smoothed particle hydrodynamics", *JOM*, **3**, 67-70.
- GINGOLD, R.A. & MONAGHAN, J.J., (1977), Smoothed particle hydrodynamics, "Theory and application to non-spherical stars", *Mon. Not. Roy. Astron. Soc.*, **181**, 375-389.
- GRANDFIELD, J, CLEARY, P., PRAKASH, M, SINNOTT, M., OSWALD, K. & NGUYEN, V, (2004), "Mathematical Modelling of Ingot Caster Filling Systems, Light Metals 2004", *Edited by A.T. Tabereaux TMS (The Minerals, Metals & Materials Society)*, 661-666.
- GRUN, G.U. and SCHNEIDER, W., (1997), "Influence of Fluid Flow Field and Pouring Temperature on Thermal Gradients in the Mushy Zone During Level Pour Casting of Billets.", *Light Metals 1997: TMS, USA*. p. 1059-1064
- GRUN, G.U. and SCHNEIDER, W., (1998), "Numerical Modelling of Fluid Flow Phenomena in the Launder- Integrated Tool Within Casting Unit Development.", *Light Metals 1998: TMS, USA*. p. 1175-1182
- HA, J., CLEARY, P. W., ALGUINE, V. and NGUYEN, T., (1999), Simulation of die filling in gravity die casting using SPH and MAGMASoft", *Proc. 2nd Int. Conf. on CFD in Minerals & Process Industries*, Melbourne, Australia, 423-428.
- MONAGHAN, J. J., (1992), "Smoothed particle hydrodynamics." *Ann. Rev. Astron. Astrophys.*, **30**, 543-574.
- PRAKASH, M., CLEARY, P. W., GRANDFIELD J., ROHAN, P. and NGUYEN, V., (2006), "Optimization of ingot casting wheel design using SPH simulations", *accepted for publication in Progress in CFD*.
- SCHNEIDER, W. and GRUN, G.U., (1995), "The New Airsol Veil Billet Casting System - Improvements, Mathematical Modelling, Cast House Experiences.", *Fourth Australian Asian Pacific Aluminium Cast House Technology Conference*. 1995: TMS. p. 296-315.